



ISSN: 0067-2904

## Near IR Photoconductive Detector Based on f-MWCNTs/Polythiophen Nanocomposite

Hawraa Sadik<sup>1</sup>, Wasan R. Saleh<sup>1\*</sup>, Naseer M. Hadi<sup>2</sup>, Noon Kadhum<sup>2</sup>

<sup>1</sup>Department of Physics, College of Science, University of Baghdad, Baghdad, Iraq.

<sup>2</sup>Laser and electro-optics research center, Ministry of Science and Technology, Baghdad, Iraq.

### Abstract

Carbon nanotubes are an ideal material for infrared applications due to their excellent electronic and photo electronic properties, suitable band gap, mechanical and chemical stabilities. Functionalised multi-wall carbon nanotubes (f-MWCNTs) were incorporated into polythiophen (PTh) matrix by electro polymerization method. f-MWCNTs/ PTh nanocomposit films were prepared with 5wt% and 10wt% loading ratios of f-MWCNTs in the polymer matrix. The films are deposited on porous silicon nanosurfaces to fabricate photoconductive detectors work in the near IR region. The detectors were illuminated by semiconductor laser diode with peak wavelength of 808 nm radiation power of 300 mW. FTIR spectra assignments verify that the thiophene groups were successfully introduced into the carbon nanotubes. SEM images reflect that the electro polymerization process gives well incorporated for the MWCNTs by PTh polymer. Characteristics of photodetector were improved after cooling the detector. Figure of merit showed a good IR radiation sensitivity and photo response, while the specific detectivity was in order of  $10^9$  cm.Hz<sup>1/2</sup>/W and at for both MWCNTs loading ratios at forward bias voltage 5 Volts. The rise time and fall time of the output signal are about 192  $\mu$ s and 121 $\mu$ s respectively which consider good values for these types of detectors.

**Keywords:** MWCNT, Polythiophen, Nano-composite, IR, Detector.

### كاشف التوصيل الضوئي للأشعة تحت الحمراء القريبة باستخدام مركب نانوي من انابيب الكربون النانوية متعددة الجدران/ بولي ثايوفين بوليمر

حوراء صادق<sup>1</sup>، وسن رشيد صالح<sup>1\*</sup>، نصير مهدي هادي<sup>2</sup>، نون كاظم<sup>2</sup>

<sup>1</sup>قسم الفيزياء، كلية العلوم، جامعة بغداد، بغداد، العراق.

<sup>2</sup>مركز ابحاث الليزر والكهرو بصريات، وزارة العلوم والتكنولوجيا، بغداد، العراق.

### الخلاصة

انابيب الكربون النانويه هي مواد مثاليه لتطبيقات الاشعه تحت الحمراء نسبه لخصائصها الالكترونيه والكهرو ضوئية الممتازه وفجوه طاقة مناسبة وثباتية الخصائص الميكانيكية والكيميائية. في هذا العمل اغشية مركبات نانويه مكونه من انابيب الكربون النانوية متعددة الجدران وبوليمر البولي ثايوفين حضرت بطريقه البلمرة الكهربائية بنسب خلط 5wt% و 10wt% من انابيب الكربون النانويه متعددة الجدران في مصفوفه البوليمر. رسبت الاغشيه على اسطح نانويه من السليكون المسامي لتصنيع كاشف توصيل ضوئي يعمل في

\*Email: wasan\_alazawi@yhaoo.com

منطقة الأشعة تحت الحمراء القريبة. اضى الكاشف بواسطة ليزر شبه الموصل الثنائي بقمه طول موجي 800nm وقدره 300mW. دراسة طيف الأشعة تحت الحمراء للاغشية المحضرة اكدت ان مجاميع الثابوتين قد اتحدت بنجاح مع انابيب الكربون النانوية. تم حساب خصائص الكاشف وقد لوحظ تحسنها بعد تبريده حيث كانت نتائج الحساسية للأشعة تحت الحمراء والريح جيدة بينما كانت قيمة الكشوفية النسبية  $\text{cm.Hz}^{1/2}/\text{W}$   $10^{+9}$  لنسبتي الخلط وعند فولتيه انحياز امامي 5 فولت. زمن نهوض و زمن هبوط الاشارة الخارجة من الكاشف كانت بحدود  $121 \mu\text{s}$  و  $192 \mu\text{s}$  على التوالي وهذا يعتبر زمن جيد لمثل هذا النوع من الكواشف.

## Introduction

An infrared detector is a transducer of radiant energy; it converts radiant energy in the infrared into a measurable form. Infrared detectors can be used for a variety of applications in the military, scientific, industrial, medical, security and automotive arenas [1]. There are two types of IR detector: photon and thermal types. In general, photon types are favored basically because of their superior sensitivity and resolution [2]. Carbon nanotubes (CNTs) are promising candidates for future IR detectors due to their unique band structure, excellent electronic, optoelectronic properties, super mechanical and chemical stabilities. They are stronger than steel, lighter than aluminum, and more conductive than copper [3, 4]. Because of these excellent properties, CNTs can be used as ideal reinforcing agents for high performance polymer composites [5]. There are two basic types of CNTs: single-wall carbon nanotubes (SWCNTs) and multi-wall carbon nanotubes (MWCNTs), which are produced using three techniques: arc discharge, laser ablation, and chemical vapor decomposition (CVD) [4]. Conjugated polymers exhibit conducting or semiconducting properties and these polymers seem to be suitable candidates due to optical and electrical properties [6]. The concept of conducting polymer was then no longer restricted for polyacetylene but extended to all other conjugated hydrocarbon and aromatic heterocyclic polymers such as polyaniline (PANI), polythiophene (PTH), poly (pphenylene) (PPP), poly (phenylene sulfide) (PPS), polypyrrole (PPY), polypyridin (PPyr). Since 1980, polythiophene has been widely used in environmentally and thermally stable conjugated polymer materials, such as chemical and optical sensors, light-emitting diodes and displays, photovoltaic devices, molecular devices, DNA detection, polymer electronic interconnects, solar cells and transistors [7, 8]. Three approaches to polymerization of thiophene: (1) electropolymerization, (2) metal-catalyzed coupling reactions, and (3) chemical oxidative polymerization. Polymers nanocomposites were first time used in 1993. Nano-composites based on conducting polymers and carbon nanotubes have gained great interest for their unique physical chemistry properties. An interesting application can be the embedding of little quantity of CNTs inside the polymer matrix of conducting polymers for the fabrication of nanocomposites which can be carried on by polymerizing the monomer in the presence of a dispersion of CNTs [8-10].

In this work an infrared photodetector was fabricated using nanocomposite based on polythiophen polymer and (COOH-MWCNTs) and characterized their physical properties.

There are many figures of merit affecting the performance of the detectors. These parameters are: responsivity ( $R_\lambda$ ), photocurrent gains (G), noise equivalent power (NEP) and the specific detectivity ( $D^*$ ). Many infrared detectors exhibit a signal which is a function of the wavelength and is sensitive only to radiation within the given spectral. This shows the range of the wavelengths over which the detector is useful. The responsivity for monochromatic light of wavelength incident normally is given by [11]:

$$R_\lambda = I_{ph}/P_{in} \quad (1)$$

where  $I_{ph}$  is the photocurrent flowing between the electrodes and  $P_{in}$  is the incident radiation power. The noise equivalent power of a detector is defined as the amount of incident flux, which gives a signal equal to the noise. For good performance the NEP should be low. This value is affected by the noise generated in the semiconductor element, and is calculated by [11]:

$$NEP = (A_d \cdot \Delta f)^{1/2} / D^* \quad (2)$$

where  $A_d$  is the detector area and  $\Delta f$  is the electrical bandwidth (Hz). Usually the specific detectivity is calculated from the responsivity  $R_\lambda$  and the noise current  $i_N$  as [11]:

$$D^*_\lambda = R_\lambda (A_d \cdot \Delta f / i_N)^{1/2} \quad (3)$$

$$i_N = (2 e I_d \Delta f)^{1/2} \quad (4)$$

$$\text{Photo response \%} = (I_1 - I_d / I_d) \times 100\% \quad (5)$$

where  $e$  is the charge of the electron,  $I_l$  is the light current and  $I_d$  is the dark current.

### Chemical Materials

The used material are functionalized multi-walled carbon nanotubes (COOH -MWCNT) which have assay 95%, length of 50 nm, outer diameter of 8-15 nm, inner diameter of 3-5 nm, COOH content: 2.56 wt% from NANOCYL S.A., Belgium. Thiophene ( $C_4H_4S$ ), acetonitrile and sodium perchlorate were purchased from Fluka with purity not less than 99%.

### Experimental Work

Crystalline silicon substrate has been employed in this work in order to prepare porous layer in the front surface of the Si wafer. Commercially n -type Si wafer of conductivity ( $\rho \leq 0.015 \Omega.cm$ ) and orientation (111) were employed as substrates. The wafer has thickness of about  $5 \pm 0.508$  mm. The samples of 1.5 x 1.5 cm dimensions were used and rinsed with methanol to remove any contamination. The photochemical etching process which used to prepare the porous silicon (PSi) samples is shown in Figure-1 After cleaning the samples they were immersed in HF acid of 50 % concentration and ethanol (1:1) in a Teflon beaker. The samples were mounted in the beaker on two Teflon tablets (plates) in such a way that the current required for the etching process could complete the circuit between the irradiated surface and the bottom surface of the Si sample. The light source is halogen lamp 250 Watt was vertically mounted by a holder above the sample, aligned and focused by quartz lens of 5 cm focal length to obtain a circular spot with a suitable power density. The photoetching irradiation time was 12 min. At the end of the photochemical etching process, the samples were rinsed with ethanol and stored in containers filled with methanol to avoid the formation of oxide layer above the produced nano spikes layer.

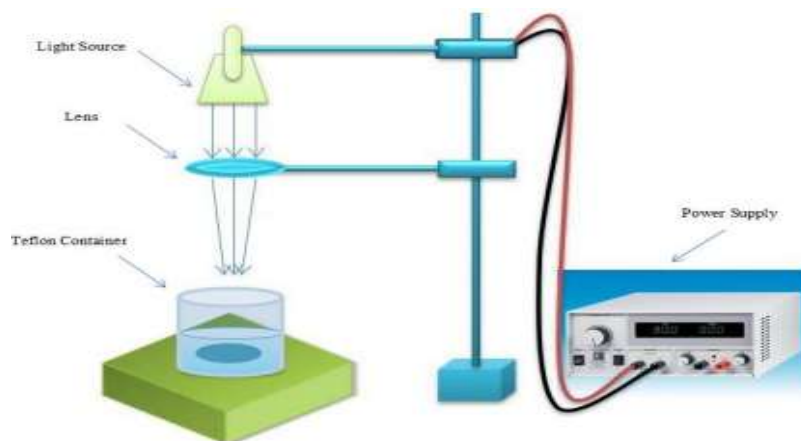


**Figure 1-** The setup of the photochemical etching process.

To prepare thiophen monomer, (0.5 M) of thiophen, (50 ml) acetonitrile and (0.1 M) of sodium perchlorite were used. Then (50 ml) of thiophen monomer was mixed with F-MWCNTs in two load ratios 5 wt% and 10 wt%. In order to prepare a thin layer of PTh/f-MWCNTs, the mixture was deposit on PSi substrate by electro polymerization which is shown in Figure-2

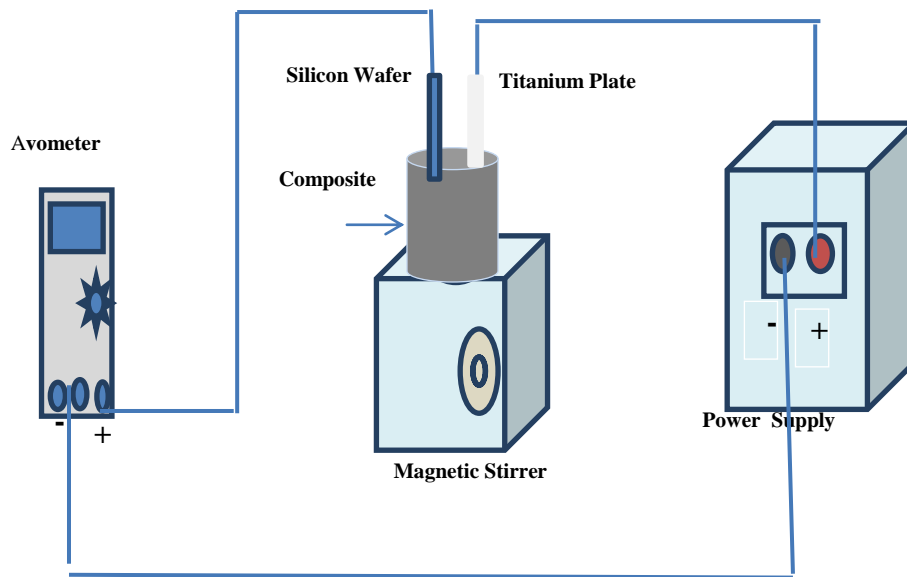


**Figure 2-** Electro polymerization process setup.

The PSi substrate was represented the anode pole, while the titanium plate represents the cathode pole. Operating voltage of 5 Volt was taken for 5 min in order to start the deposition process. After completing the growing of thin film, the film leaves to dry in atmosphere for around 15 min. The micro mask of 0.4 mm electrode and distance between the two electrodes is 0.9 cm, illustrated in Figure-3a was used to deposit the Aluminum (Al) electrical electrodes on the film surface by the evaporation technique. The copper wires were used to connect the electrodes to the operation electrical circuit by the aid of silver paste. Figure-3b illustrated the final shape for the fabricated photoconductive detector such as consider in [12].

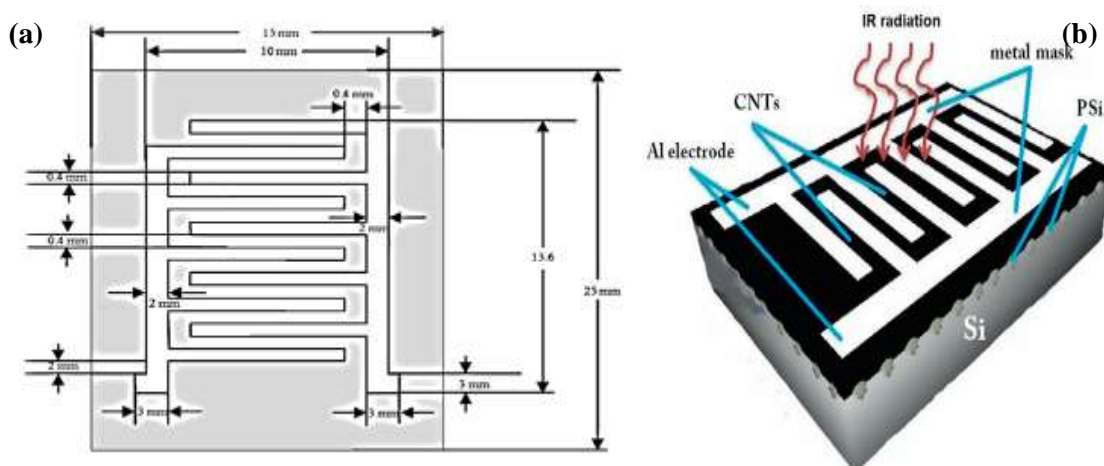


**Figure 3-** (a) Schematic diagram of the IDE masks utilized in this work, (b) Final shape for the fabricated photoconductive detector [12].

A suitable setup was used to investigate the detector’s parameters, such as, I-V characteristics, figures of merit and the response time of the fabricated infrared detectors. Figure-4 shows the setup for

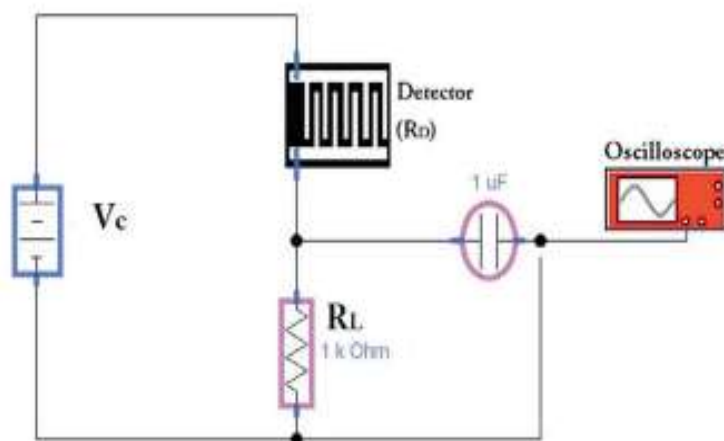


**Figure 4-** The operation circuit diagram of Infrared photoconductive detector [12].

## Results and Discussion

Morphological, optical, and electrical properties were measured to characterize the prepared PTh/f-MWCNTs films and for the fabricated IR photoconductive detectors.

### FTIR Analysis

Fourier Transform Infrared Spectroscopy (IR-prestige 21, Shimadzu) was used to determine the chemical components and absorption band of prepared material.

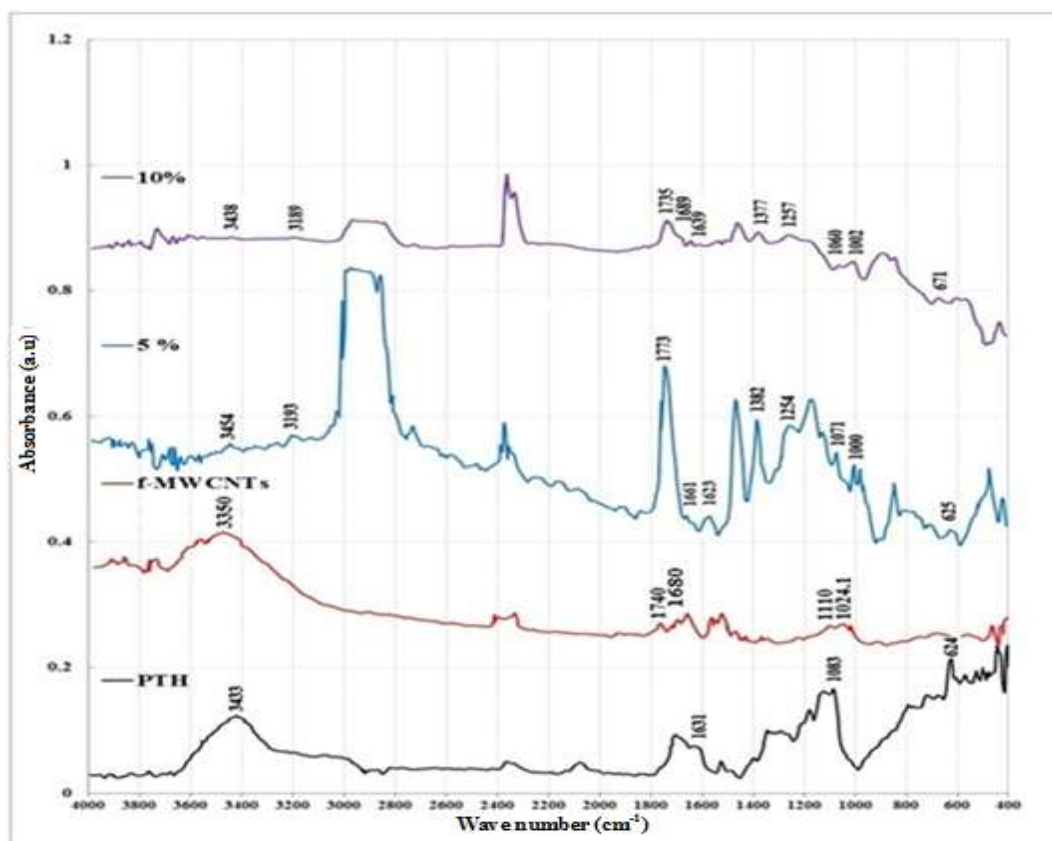


**Figure 5-** FTIR spectra of: bulk PTh powder, f-MWCNTs, PTh-5wt% f-MWCNTs and PTh-10wt% f-MWCNTs.

Figure-5 shows the FTIR spectrum of electro-polymerized polythiophene (bulk PTh powder). The major peaks at  $624\text{ cm}^{-1}$ ,  $1083\text{ cm}^{-1}$ ,  $1631\text{ cm}^{-1}$  and  $3433\text{ cm}^{-1}$  indicate the presence of C=C, C-S, C-C and C-H bonds in polythiophene respectively. This result is very close to the standard FTIR spectrum of polythiophene and totally different from that of monomer thiophene, which confirms the successful

polymerization of thiophene monomer and formation of polythiophene. The major peaks of COOH-MWCNTs appear at  $3350\text{ cm}^{-1}$ ,  $1740\text{ cm}^{-1}$ ,  $1680\text{ cm}^{-1}$ ,  $1110\text{ cm}^{-1}$ ,  $1024.1\text{ cm}^{-1}$  indicate the presence O-H, C=O, C=C, C-O, C-C bonds. The FTIR spectrums for PTH/COOH-MWCNTS composites in 5 wt% and 10 wt% load ratio respectively. In these figures an O-H bond is found around  $(3438-3454)\text{ cm}^{-1}$ , the stretching vibration absorbance of C=O in carboxylic acid appeared at  $(1735-1773)\text{ cm}^{-1}$  and at approximately  $(3189-3193)\text{ cm}^{-1}$  characteristic of C-H stretch was observed due to alcoholic or phenolic or carboxylic groups. Around  $(1623-1639)\text{ cm}^{-1}$  C-C bond was observed,  $(1689-1661)\text{ cm}^{-1}$  C=C bond of PTh was appeared, while around  $(1377-1382)\text{ cm}^{-1}$  S=O bond represent the finger print of composite. The following bonds were also observed; the peak at  $(1257-1254)\text{ cm}^{-1}$  C-O stretch, the peaks at  $(1060-1071)\text{ cm}^{-1}$  C-C stretch,  $(1002-1000)\text{ cm}^{-1}$  assigned to C-S stretching, in  $(671-625)\text{ cm}^{-1}$  C=C bond of PTH was appeared, These FTIR spectra assignments verify that the thiophene groups were successfully introduced into the carbon nanotubes.

### Morphological Studies

The field emission on scanning electron microscope (SEM) technique from Hitachi FE-SEM model S-4160 and Oxford instrument, Inca-SEM model 7353, have been applied to study the morphology of the deposited F-MWCNTs, PTH, and PTH/MWCNT films.

Figure-6 (a) shows that PTH polymer, deposited on titanium plate by electropolymerization, takes like flower shape. Figure-6 (b) shows that the SEM images for the MWCNTs is very smooth and like spaghetti. From Figures – 6(c) and (d) one can observed that MWCNTs are compactly adhered onto the shell of functional MWCNTs compared to Figure -6a. It shows the incorporation of MWCNTs into the PTh leafs, so the SEM analysis revealed the interaction of MWCNTs with polymer matrix because the presence of a random network of interconnected bundles of MWCNT, packed underneath the polymer confirm formation of polymer nanocomposite. This result is in a good agreement with Massoumi et al. [13].

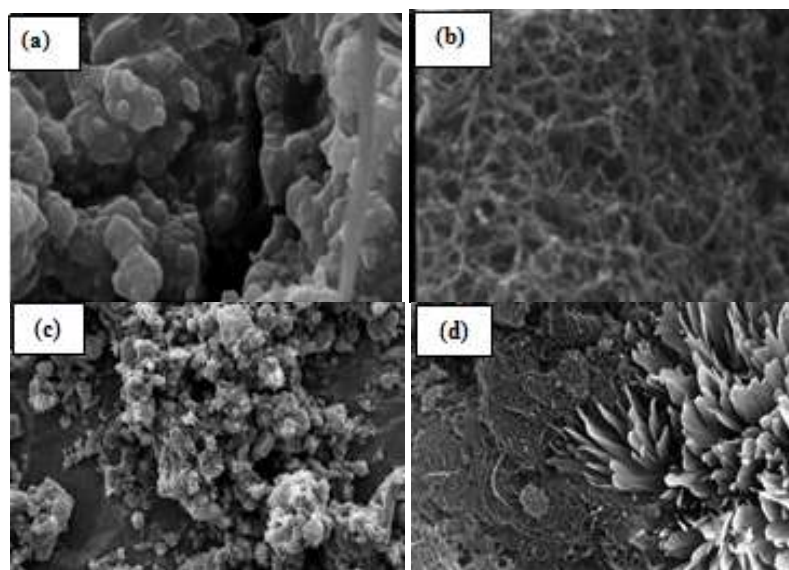


**Figure 6-** SEM images of: (a) Polythiophen polymer deposited by electro-polymerization method, (b) f-MWCNTs, and (c and d) PTh/f-MWCNTs nanocomposite of 5wt% load ratio and magnification of:  $10\text{ }\mu\text{m}$  and  $1\text{ }\mu\text{m}$  respectively.

### I-V Characteristics and figures of Merits

Figures- (7-9) show the current-voltage (I-V) characteristics of the fabricated photoconductive detector as a function of forward bias voltage at dark and under illumination of laser diode of 808 nm wavelength and 300mW radiation power. It is clear that the device has low sensitivity and increased gradually at low bias voltages ( $<2.5\text{ volt}$ ) and this sensitivity increased exponentially with increasing of bias voltage ( $>2.5\text{ volt}$ ). The mechanism of the IR photocurrent is related to the IR absorption in CNTs, exciton generation and their dissociation on photoelectrons and photo holes at the metallic electrode- nanotubes interface



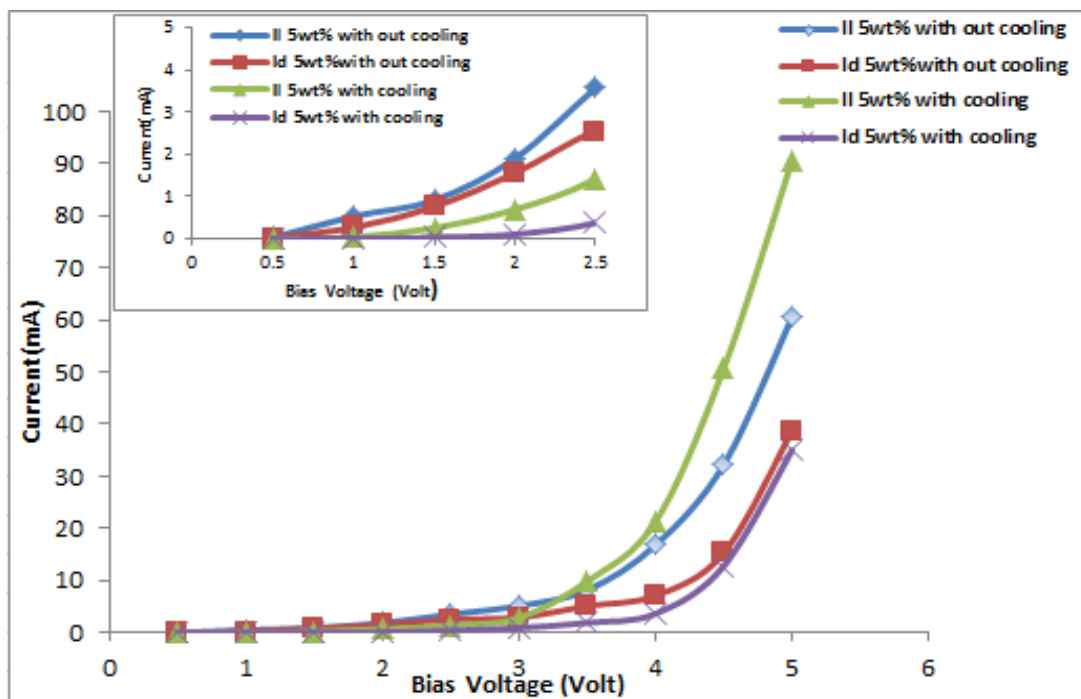


**Figure 7-** I-V characteristics of the PTh/ MWCNTs film with concentration 5 wt% of MWCNTs illuminated by laser diode of 808 nm wavelength and 300 mW radiation power with and without cooling, inset: I-V curves between 0.5-2.5 Volt.

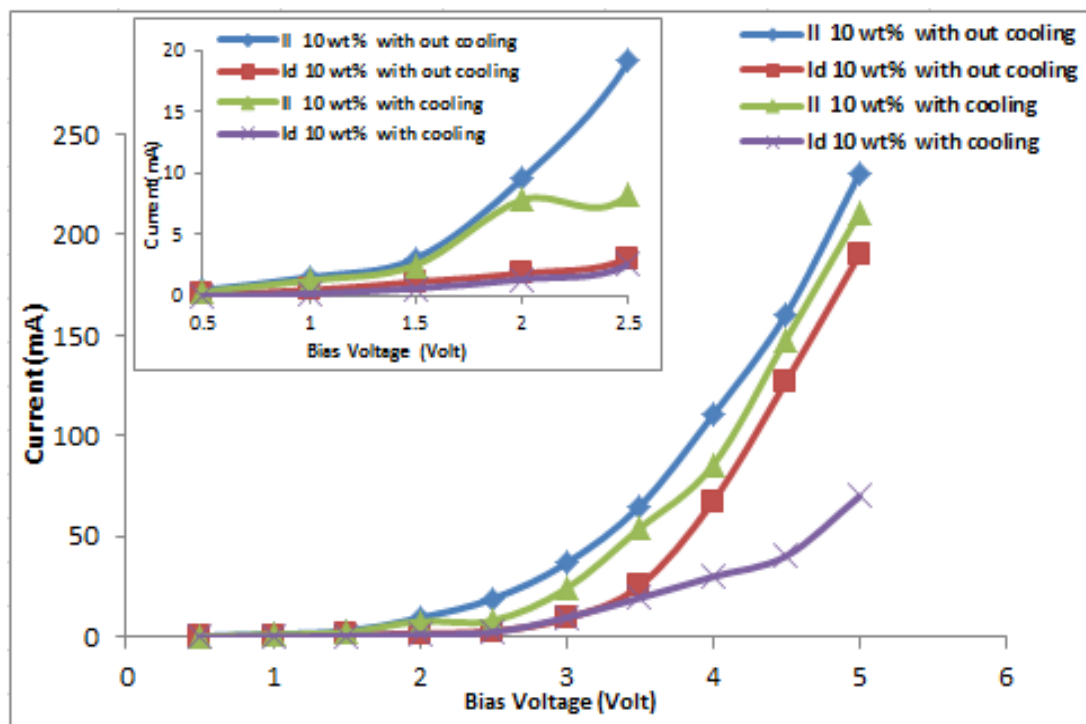


**Figure 8-** I-V characteristics of the PTh/ MWCNTs film with concentration 10 wt% of MWCNTs illuminated by laser diode of 808 nm wavelength and 300 mW radiation power with and without cooling, inset: I-V curves between 0.5-2.5 Volt.

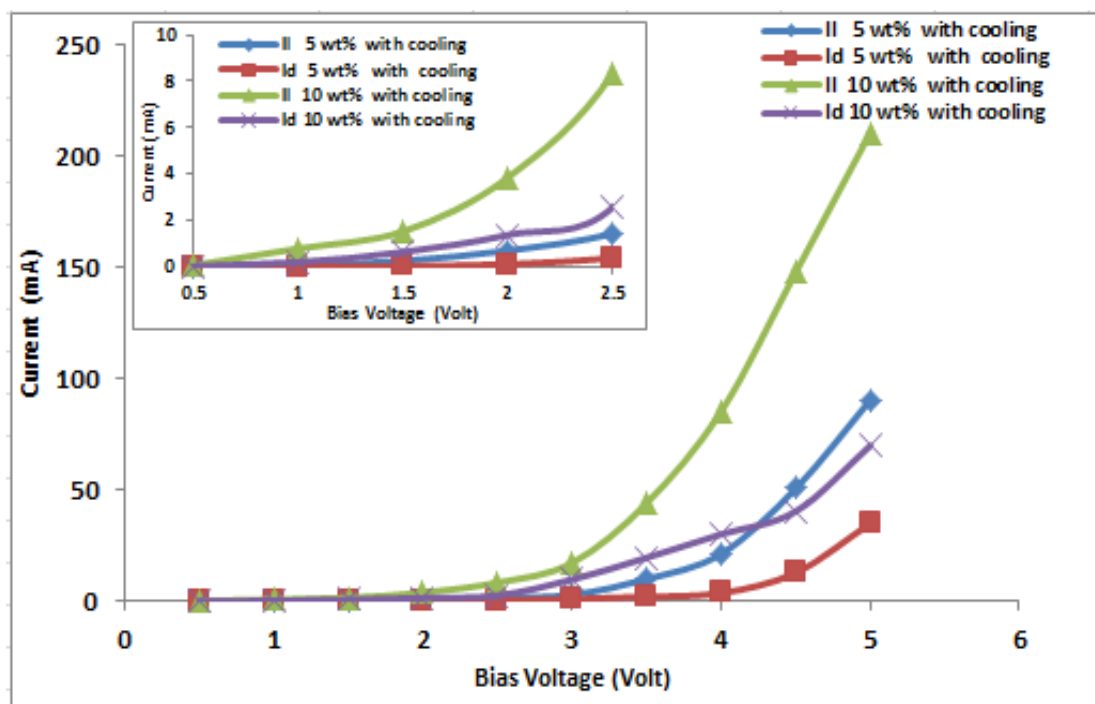


**Figure 9-** I-V characteristics of the PTH/ MWCNTs film with concentrations 5 wt% and 10wt% of MWCNTs illuminated by laser diode of 808 nm wavelength and 300 mW radiation power with cooling, inset: I-V curves between 0.5-2.5 Volt.

When the laser light is illuminated at the interface, some energetic electrons overcome the symmetric tunnel barrier at the interface and fall into the metal electrode leaving holes in the film. This causes an electron hole separation at the interface and thereby creates a local electric field. Under the influence of this electric field, the carrier, and then diffuses to the other electrode through percolating CNTs network [14].

Under illumination of IR radiation, the sensitivity of the detector with loading ratio 5% with cooling is higher than that for the detectors without cooling as in Figure-7, while for load ratio 10% of CNTs cooling the detector decreasing the noise of the detector (dark current) as clear in Figure-8. It is obvious from the figures that the photo current of two loading ratio without cooling is unstable and become stable under cooling to about 7 °C less than room temperature. This is may be attributed to heat that generated by thermal fluctuations in conducting materials from the random motion of electrons in a conductor. The electrons are in constant motion, colliding with each other and with the atoms of the material. Each motion of an electron between collisions represents a tiny current. The sum of all these currents taken over a long period of time is zero. Since by cooling, the traps will decreased which lead to increase the useful electrons transitions and decrease the thermal noise. So, the main effect of cooling the detectors are to increase the responsivity as associated with increased photoresponse and reduce the noise processes associated with thermal generation.

Photocurrent detectors typically need to be cooled, either to move their response further into the IR where the signal of interest is present or to provide stability. So the result of I-V characteristics with cooling is more stable than that without cooling and the sensitivity increasing with increasing the concentration of CNTs, which in term leads to improve the figures of merit of the detector as tabulated in Table-1. It is clear that increasing the load ratio and cooling the detectors improved the characteristics of detectors in about 2-3 times. The table revealed that each of the responsivity, quantum efficiency, specific detectivity and the photo-response were increase while the NEPA value was decreased with increasing of concentration of CNTs and cooling the detector. A photo-response of 201%, and NEP of  $5.33 \times 10^{-10}$  W with specific detectivity of  $1.88 \times 10^{+9}$  (cm.Hz<sup>1/2</sup>)/W consider a good values for this type of detectors in near IR region.



**Table 1-** Figures of merit of photodetectors (calculated using equations 1-5) with loading ratio 5 wt% and 10 wt% of CNTs at forward bias voltage 5 V, using 300 mW semiconductor laser diode with peak wavelength of 808 nm.

Sample case	$R_{\lambda}$ (A/W)	Q.E.	NEP (Watt)	$D^*$ (cm.Hz <sup>1/2</sup> )/W	Photo-response %
5 wt% without cooling	0.080	0.122	$1.38 \times 10^{-9}$	$7.25 \times 10^{+8}$	57.894
5 wt% with cooling	0.120	0.185	$8.77 \times 10^{-10}$	$1.14 \times 10^{+09}$	158.5
10 wt% without cooling	0.306	0.471	$8.04 \times 10^{-10}$	$1.24 \times 10^{+9}$	21.094
10 wt% with cooling	0.280	0.431	$5.33 \times 10^{-10}$	$1.88 \times 10^{+9}$	201

The figures of merit enhanced for many reasons: (1) the matrix method which is used in growing the films gave best results in compared with those films prepared in other methods, (2) PTh polymer have good conductivity, (3) cooling the detector increasing the stability and decreases the noise of the detector (dark current). In general the results of using the matrix method in growing the films gave best results in compared with those films prepared in other methods [13, 14].

#### Rise and fall times

The response time of the fabricated PTh/f-MWCNTs IR photoconductive detector with loading ratio 5 wt% of CNTs is tested by illuminated the detector with laser of 808nm wavelength and incident power 300 mW. The trace of the output pulse, illustrated in Figure- 10, was carried out by digital storage oscilloscope (UNI-T UT2202C) of 200 MHz band widths, while the chopping frequency was 3000 Hz.

It can be noticed from the output signal that the rise time 10% -90% is in the order of 192  $\mu$ s and the fall time (1-1/e) is about 121  $\mu$ s, while the recovery time is about 80 $\mu$ s. This response speed can consider better than the results in other works [12, 15, 16].



**Figure 10-**The output signal from PTh/f-MWCNT with load ratio 5wt% of CNTs photoconductive detector illuminated with IR radiation from diode laser of 808nm wavelength and incident power of 300 mW.

#### Conclusions

Infrared photoconductive detectors based on nanocomposite of MWCNTs in different load ratio with polythiophen conductive polymer work in the near IR region were fabricated. The films prepared by electropolymerization on PSi substrate. SEM images and FTIR reflect that the electropolymerization process gives very good coating for the CNTs by polythiophen polymer. Using matrix method in growing the films as well as detector cooling enhanced the figures of merit in about 2-3 times. The rise time and fall time are highly improved and consider acceptable for this type of detectors.

### Acknowledgments

The authors would like to thanks Dr. Abdulkareem M. Ali from department of chemistry, college of science in Baghdad University and Miss. Ghaida Hamza from laser and electro-optics research center in Ministry of Science and Technology for their assistant during the work.

### References

1. Kumar, K. D. **2015**. Infrared Quantum Dot Detectors. *GJRA - GLOBAL Journal for research analysis*, **4**: 63-66.
2. Edwards, M. E., Batra, A. K., Chilvery, A. K., Guggilla, Curley, P. M., Aggarwal, M. D. **2012**. Pyroelectric properties of PVDF: MWCNT nanocomposite film for uncooled infrared detectors. *Materials Sciences and Applications*, **3**: 851-855.
3. Zeng, Q., Wang, S., Yang, L., Wang, Z., Pei, T., Zhang, Z., Peng, L-M., Zhou, W., Liu, J., Zhouand, W., Xie, S. **2012**. Carbon nanotube arrays based high-performance infrared photodetector. *Opt. Mat. Exp.* **2**: 839-848.
4. Tonpheng, B. **2011**. Thermal and mechanical studies of carbon nanotubepolymer composites synthesized at high pressure and high temperature. Doctoral Thesis, Department of physics University of Umeå, Sweden Umeå,
5. Gopal Sahoo, N., Rana, S., Whan Cho, J., Lia, L., Hwa Chana, S. **2010**. Polymer nanocomposites based on functionalized carbon nanotubes. *Polymer Science*, **35**: 837–867.
6. Tiwari, D., Sen, V. and Sharma, R. **2012**. Tempreature dependent studies of electric and dielectric properties of polythiophen based nano composite. *Journal of pure and applied physics*, **50**: 49-56.
7. Deshpande, M. D., Kondawar, S. B. **2014**. Electrical conductivity of multi-walled carbon nanotubes doped conducting polythiophene. *IJRASET*. **2**. Issue X.
8. Chen, L. R. & Ping, L. Z. **2009**. Polythiophene: Synthesis in aqueous medium and controllable morphology. *Chinese Science Bulletin*. **54**, 2028-2032.
9. Iqbal, T., Ali, W. **2015**. Synthesis and characterization of carbon based polymer nanocomposites for enhanced conductivity. *Journal of Ovonic Research*. **11**: 293 – 301
10. Parija, B. K., Biswal, C. R., Sahoo, P. K., Dash, M. P., Adhikary, M. C., Nayak, P. L. **2013** Synthesis and Characterization of Poly (Flouroaniline)/MWCNT Composite . *IJES*. **2**: 133-14.
11. Keys, R. J. **1980**. *In Optical and Infrared Detectors, Topics in Applied Physics*. Second edition, 19, Springer-Verlag, USA.
12. Wasan, R. S. **2015**. A carbon nanotubes photoconductive detector for middle and far infrared regions based on porous silicon and a polyamide nylon polymer. *Eur. Phys. J. Appl. Phys.* **7**, 30401-1, DOI: 10.1051
13. Massoumi, B., Jaymand, M., Samadi, R., Entezami, A. A. **2014**. In situ chemical oxidative graft polymerization of thiophene derivatives from multi-walled carbon nanotubes. *J. Polym. Res.*, **21**: 442
14. Naje, A. N., Noori, O. A. **2015**. Carbon Nanotubes Photoconductive Detector in Near- Infrared Region. *IJAIEEM*, **4**: 105-108.
15. Marwa, Abdul Rahman. **2015**. Fabrication of Carbon Nanotubes Detector for IR Laser. Master Thesis, College of Science for Women – University of Baghdad.
16. Abdulla, M. Suhail. **2013**. Carbon nanotubes -porous silicon high sensitivity infrared detector. *IJSR*, **2**: 209-210.